Fluid-Antenna Array Enabled DOA Estimation for the Hybrid Analog-Digital Architecture with Unknown Nonuniform Noise

Jiaji Ren[†], Ye Tian[†], Tuo Wu[◇] and Wei Liu[§]
[†]*Faculty of Electrical Engineering and Computer Science, Ningbo University, Ningbo, China*
[◇]*School of Electrical and Electronic Engineering, Nanyang Technological University, Singapore*
[§]*Department of Electrical and Electronic Engineering, Hong Kong Polytechnic University, Hong Kong, China*

***Abstract*—The fluid antenna (FA) array leverages the spatial degrees of freedom in constrained environments while significantly reducing hardware layout complexity and costs. In this paper, an FA array enabled direction-of-arrival (DOA) estimation method for the hybrid analog-digital (HAD) architecture under the nonuniform noise is proposed. In this setup, the antenna array is moved to different positions within the constrained area, the corresponding received signals are collected, and then enabling high-precision and low-cost DOA estimation. Different from existing approaches using the HAD array output directly, an efficient covariance matrix reconstruction scheme is first exploited to recovers the large-scale array covariance matrix; and then, the iterative least-squares subspace estimation (ILSSE) technique is applied to eliminate the unknown uniform noise; finally, the the multiple signal classification (MUSIC) algorithm is applied for DOA estimation. Simulation results validate the superiority and effectiveness of this approach in terms of both accuracy and efficiency.**

***Index Terms*—Fluid antenna (FA) array, hybrid analog-digital (HAD) architecture, direction-of-arrival (DOA) estimation, covariance matrix reconstruction, nonuniform noise.**

I. Introduction

The sixth-generation (6G) mobile communication system is widely regarded as providing revolutionary support for future communications [1]. It is expected to achieve data transmission rates at the Terabits per second (Tbit/s) level, and support centimeter-level positioning accuracy to meet the demands of emerging applications such as autonomous driving, immersive interactive experiences, and virtual reality [2]. As a key sensing technology, direction-of-arrival (DOA) estimation plays a crucial role in enabling these applications and meeting the associated requirements [3].

To meet the ultra-high accuracy requirements for estimation in various future application scenarios, massive multiple input multiple output (M-MIMO) or ultra-massive MIMO antenna arrays are typically deployed at sensing nodes such as radars and base stations (BSs), leveraging their high spatial resolution advantages. However, various hardware limitations hinder the application of traditional fully-digital array [4]. To address this issue, the hybrid analog-digital (HAD) architecture has become an effective solution, which maintains system performance while reducing the number of radio frequency (RF) chains. This approach has been widely studied in [5]–[8].

Fluid antenna (FA) technology is an emerging approach to enhance full-space performance, enabling flexible adjustment of antenna positions in certain continuous space to better exploit spatial degrees of freedom (DoFs), in comparison with the traditional fixed position antenna (FPA) arrays [9]–[14]. So far, several FA enabled methods have been proposed to demonstrated their advantages in wireless sensing [15]–[17], such as enhancing beamforming design, spectrum sensing and secure wireless communication, etc. However, it is necessary to point out that less attention has been paid on DOA estimation. As a major focus for future advancements in FA, DOA estimation technologies enabled by FA will be essential in fields such as wireless communication, radar, and sonar detection, offering considerable potential value.

In this paper, a DOA estimation method enabled by an FA array in the presence of unknown nonuniform noise is proposed. In comparison with uniform noise, unknown nonuniform is more likely to affect the separation between the signal and noise subspaces, leading to a more serious impact on DOA estimation [18]–[20]. Unlike the antenna movement patterns in most existing FA systems, we employ an array-level mobility approach combined with hybrid analog-digital connections, which can significantly reduce both hardware overhead and the complexity of physical movement implementation. By utilizing observation data from different positions to reconstruct the covariance matrix of the equivalent digital antenna array, and applying the iterative least-squares subspace estimation (ILSSE) technique to eliminate nonuniform noise, an improved DOA estimation is finally provided by the MUSIC algorithm is applied. Simulation results demonstrate the effectiveness of the proposed method efficiently.

II. System Model

As shown in Fig. 1, we consider the application of FAs in the uplink of a wireless communication system. In this configuration, the BS deploys a FA array with the capability to freely adjust the array's position, and a sub-connected HAD architecture is used to connect the antenna array with the RF chains for DOA estimation of L users. We adopt an array-level mobility approach, where the N FAs within the array move synchronously along a 1-D DOA within the confined region.

This work was partially supported by the Zhejiang Provincial Natural Science Foundation of China under Grant LY23F010004, and the Natural Science Foundation of Ningbo Municipality under Grant 2024J232.

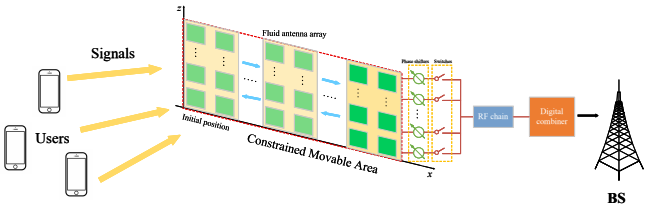

Fig. 1. FA array-assisted HAD architecture.

Assume that the FA array moves K times for spatial sampling, then the received signal at the k-th position can be expressed as

$$\mathbf{\Upsilon}_k = \mathbf{H}_k \mathbf{P}^{1/2} \mathbf{S} + \mathbf{N}_k \tag{1}$$

where $\mathbf{S}$ stands for the transmitted pilot symbol matrix, the pilot symbols are orthogonal to each other, satisfying $\mathbf{S}\mathbf{S}^H = \mathbf{I}_L$. $\mathbf{P}^{1/2} = \operatorname{diag}\left\{\sqrt{p_1}, \ldots, \sqrt{p_L}\right\}$ is the power matrix, which encapsulates the transmission power of each user. $\mathbf{N}_k$ is the zero-mean additive Gaussian nonuniform noise, whose each row obeys $\mathbf{n} \sim \mathcal{CN}(0, \mathbf{Q})$. $\mathbf{Q} = \operatorname{diag}\left\{\sigma_1^2, \ldots, \sigma_N^2\right\}$ is the noise covariance matrix, where σ_n^2 corresponds to the noise power at the n-th sensor.

For simplicity, we consider the line-of-sight (LoS) propagation scenario and adopt a channel model based on far-field responses. Additionally, we focus on a quasi-static fading block, where the position changes of the FA array do not affect the DOA and the magnitude of the complex coefficients for each channel path. With these reasonable assumptions, the channel matrix from the user to the FA array can be expressed as $\mathbf{H}_k = \mathbf{A}_k \mathbf{\Lambda}$, where $\mathbf{\Lambda} = \operatorname{diag}\{\gamma_1, \cdots, \gamma_L\}$ consists of the path gains of complex multipath channel. $\mathbf{A}_k$ represents the array manifold matrix, which varies with the position of the FA array. The array manifold matrix at the k-th position of the FA array can be expressed as

$$\mathbf{A}_k = \left[\mathbf{a}_k(\theta_1, \phi_1), \cdots, \mathbf{a}_k(\theta_L, \phi_L)\right]. \tag{2}$$

In specific, the FA array is configured as a uniform planar array (UPA) composed of $N_x \times N_z$ FAs, whose corresponding array manifold vector can be expressed as

$$\mathbf{a}_k(\theta_\ell, \phi_\ell) = \mathbf{a}_{k,x}(\theta_\ell, \phi_\ell) \otimes \mathbf{a}_{k,z}(\theta_\ell, \phi_\ell) \tag{3}$$

with

$$\begin{aligned}\mathbf{a}_{k,x}(\theta_\ell, \phi_\ell) = &[e^{j2\pi d_x \sin\theta\cos\phi/\lambda}, \cdots, \\ &\cdots, e^{j2\pi((N_x-1)d+d_k))\sin\theta\cos\phi/\lambda}]^T\end{aligned} \tag{4}$$

$$\mathbf{a}_{k,z}(\theta_\ell, \phi_\ell) = \left[1, \ldots, e^{j2\pi(N_z-1)d\sin\phi/\lambda}\right]^T \tag{5}$$

where $\otimes$ denotes the Kronecker product, λ refers to the carrier wavelength, $d = \lambda/2$ the inter-element spacing, and d_k the distance from the initial position.

Defining the equivalent transmitted signal $\bar{\mathbf{S}} = \mathbf{\Lambda}\mathbf{P}^{1/2}\mathbf{S}$, we can rewrite the received signal in (1) as

$$\mathbf{\Upsilon}_k = \mathbf{A}_k \mathbf{\Lambda} \mathbf{P}^{1/2} \mathbf{S} + \mathbf{N}_k = \mathbf{A}_k \bar{\mathbf{S}} + \mathbf{N}_k. \tag{6}$$

Consequently, by summing the received signals of the FA array at K positions, we can obtain the received signal of the equivalent large virtual array as

$$\mathbf{\Upsilon} = \mathbf{A}\bar{\mathbf{S}} + \mathbf{N} \tag{7}$$

where $\mathbf{\Upsilon} = \left[\mathbf{\Upsilon}_1^T, \ldots, \mathbf{\Upsilon}_K^T\right]^T$, $\mathbf{A} = \left[\mathbf{A}_1^T, \ldots, \mathbf{A}_K^T\right]^T$, and $\mathbf{N} = \left[\mathbf{N}_1^T, \ldots, \mathbf{N}_K^T\right]^T$.

Denote $\mathbf{R}$ to be the spatial covariance matrix (SCM) of virtual array, then the overall SCM can be divided into

$$\mathbf{R} = \mathbb{E}\{\mathbf{\Upsilon}\mathbf{\Upsilon}^H\} = \begin{bmatrix} \mathbf{R}_{1,1} & \mathbf{R}_{1,2} & \cdots & \mathbf{R}_{1,K} \\ \mathbf{R}_{2,1} & \mathbf{R}_{2,2} & \cdots & \mathbf{R}_{2,K} \\ \vdots & \vdots & \ddots & \vdots \\ \mathbf{R}_{K,1} & \mathbf{R}_{K,2} & \cdots & \mathbf{R}_{K,K} \end{bmatrix} \tag{8}$$

where $\mathbf{R}_{k_1,k_2} = \mathbb{E}\{\mathbf{\Upsilon}_{k_1}\mathbf{\Upsilon}_{k_2}^H\} \in \mathbb{C}^{N\times N}$ is the sub-SCM of virtual array. We can utilize $\mathbf{R}$ along with subspace algorithms for DOA estimation. However, the signal received by the FA array undergoes selection, analog combining and sampling. As a result, the final output of the FA array can be given by

$$\mathbf{Y} = \left[\mathbf{Y}_1^T, \ldots, \mathbf{Y}_K^T\right]^T \tag{9}$$

where $\mathbf{Y}_k = \mathbf{w}_k^H \mathbf{\Upsilon}_k$ represents the output of the FA array at the k-th position. $\mathbf{w}_k = \mathbf{s}_k \odot \mathbf{m}_k$ is the analog combining vector with $\odot$ standing for the Hadamard product. $\mathbf{s}_k$ is a binary switch vector that represents the selection function of the switches. $\mathbf{m}_k = \left[e^{j\alpha_{k,1}}, \ldots, e^{j\alpha_{k,N}}\right]$ is the phase shift vector, with $0 \le \alpha_{k,n} \le 2\pi$ denoting the phase shift coefficient of the phase shifter.

It can be seen that although the use of the HAD architecture reduces hardware overhead, the array scale is reduced significantly, preventing us from obtaining the SCM $\mathbf{R}$ of the virtual array directly. In what follows, we will first introduce an efficient method to reconstruct a SCM, and then apply it for satisfactory DOA estimation.

III. Proposed Method

Denote $\hat{\mathbf{R}}_{k_1,k_2}$ as the reconstructed submatrix corresponding to the block $\mathbf{R}_{k_1,k_2}$. We first reconstruct the diagonal elements of the sub-covariance matrix. When reconstructing the n-th diagonal element, only the n-th FA is connected, and the phase shift coefficient of the phase shifter is adjusted to 0. At this point, the analog combining vector $\mathbf{w}$ will be a vector of all zeros, with only the n-th position set to 1. Define $\mathbf{b}_n$ as a vector of all zeros except for the n-th position, which is 1, i.e., $\mathbf{b}_n = [0, 0, \cdots, 1, \cdots, 0]^T$, where the 1 is at the n-th entry. Then the n-th diagonal element of $\mathbf{R}_{k_1,k_2}$ can be reconstructed as

$$\hat{\mathbf{R}}_{k_1,k_2}(n,n) = \mathbf{b}_n^H \mathbf{R}_{k_1,k_2} \mathbf{b}_n = R_{n,n} \tag{10}$$

and the remaining $N^2 - N$ elements appear in pairs. For each pair of off-diagonal symmetric elements $\mathbf{R}_{k_1,k_2}(n,m)$ and $\mathbf{R}_{k_1,k_2}(m,n)$, we solve them jointly. Reconstructing this pair of elements requires two transformations of the analog combining vector vector. In the first transformation, we only connect the n-th and m-th ($1 \le n \ne m \le N$) FAs, and set the

phase shift coefficients of the phase shifters at both antennas to 0. At this point, the analog combining vector $\mathbf{w}$ will be a vector of all zeros, with only the n-th and m-th position set to 1, which can be expressed by $\mathbf{b}_m + \mathbf{b}_n$. We than have

$$\begin{aligned} R_{n,m} &= (\mathbf{b}_n + \mathbf{b}_m)^H \mathbf{R}_{k_1,k_2}(\mathbf{b}_n + \mathbf{b}_m) \\ &= \mathbf{R}_{k_1,k_2}(n,n) + \mathbf{R}_{k_1,k_2}(n,m) + \mathbf{R}_{k_1,k_2}(m,n) \\ &\quad + \mathbf{R}_{k_1,k_2}(m,m) \end{aligned} \tag{11}$$

In the second transformation, the phase shift coefficients of the phase shifters connected to the n-th and m-th antennas are adjusted to α and $-\alpha$, $\alpha \in \left(0, \frac{\pi}{2}\right)$, respectively. At this point, the analog combining vector $\mathbf{w}$ can be expressed as $\mathbf{b}_m e^{-j\alpha} + \mathbf{b}_n e^{j\alpha}$, we have

$$\begin{aligned} R_{m,n} &= (\mathbf{b}_m e^{-j\alpha} + \mathbf{b}_n e^{j\alpha})^H \mathbf{R}_{k_1,k_2}(\mathbf{b}_m e^{-j\alpha} + \mathbf{b}_n e^{j\alpha}) \\ &= \mathbf{R}_{k_1,k_2}(n,n) + e^{-j2\alpha}\mathbf{R}_{k_1,k_2}(n,m) \\ &\quad + e^{j2\alpha}\mathbf{R}_{k_1,k_2}(m,n) + \mathbf{R}_{k_1,k_2}(m,m). \end{aligned} \tag{12}$$

Since the diagonal elements of $\mathbf{R}_{k_1,k_2}$ have already been obtained in advance based on (10), we can simplify and solve equations (11) and (12) simultaneously via

$$\begin{cases} e^{-j2\alpha}\mathbf{R}_{k_1,k_2}(n,m) + e^{j2\alpha}\mathbf{R}_{k_1,k_2}(m,n) = \widetilde{R}_{m,n} \\ \mathbf{R}_{k_1,k_2}(n,m) + \mathbf{R}_{k_1,k_2}(m,n) = \widetilde{R}_{n,m} \end{cases} \tag{13}$$

Equation (13) admits the following matrix-vector representation

$$\mathbf{E}\mathbf{r}_n = \mathbf{c}_n \tag{14}$$

where $\mathbf{E} = \begin{bmatrix} e^{-j2\alpha} & e^{j2\alpha} \\ 1 & 1 \end{bmatrix}$, $\mathbf{r}_n = \begin{bmatrix} \mathbf{R}_{k_1,k_2}(n,m) \\ \mathbf{R}_{k_1,k_2}(m,n) \end{bmatrix}$ and $\mathbf{c}_n = \begin{bmatrix} \widetilde{R}_{m,n} \\ \widetilde{R}_{n,m} \end{bmatrix}$. It is clear that by ensuring $e^{j2\alpha} \neq e^{-j2\alpha} \neq 1$, we can obtain a non-singular invertible matrix $\mathbf{E}$. Then, the closed-form expression for the reconstructed off-diagonal elements of $\mathbf{R}_{k_1,k_2}$ can be written as

$$\begin{cases} \hat{\mathbf{R}}_{k_1,k_2}(n,m) = \rho(\widetilde{R}_{m,n} - e^{j2\alpha}\widetilde{R}_{n,m}) \\ \hat{\mathbf{R}}_{k_1,k_2}(m,n) = \rho(e^{-j2\alpha}\widetilde{R}_{n,m} - \widetilde{R}_{m,n}) \end{cases} \tag{15}$$

where $\rho = 1/(e^{-j2\alpha} - e^{j2\alpha})$.

By iterating n and m from 1 to N, we can reconstruct all the elements of the sub-SCM. Subsequently, according to (8), we aggregate all sub-SCMs to obtain a $NK \times NK$ matrix $\hat{\mathbf{R}}$. By comparing to an FPA array with the same number of physical antennas, the dimensionality of reconstructed SCM is expanded by a factor of K, allowing for the resolution of more DOAs and more accurate estimation performance.

With available $\hat{\mathbf{R}}$, we next to eliminate the impact of unknown nonuniform noise. The ILSSE technique is exploited here, whose corresponding object function can be formulated as the following optimization problem

$$\min_{\mathbf{Q}} \|\hat{\mathbf{R}} - \mathbf{A}\mathbf{R}_{\mathbf{s}}\mathbf{A}^H - \mathbf{Q}\|_F^2 \tag{16}$$

where $\|\cdot\|_F^2$ denotes the Frobenius norm, $\mathbf{R}_{\mathbf{s}}$ represents the signal covariance matrix.

Note that $\mathbf{A}$ and $\mathbf{Q}$ are unknown variables, to solve formulation (16) efficiently, we rewrite it as

$$\min_{\mathbf{U},\mathbf{Q}} \|\hat{\mathbf{R}} - \mathbf{U}\mathbf{U}^H - \mathbf{Q}\|_F^2 \tag{17}$$

where $\mathbf{U}$ denotes the signal subspace which spans the same column space as $\mathbf{A}$.

The alternating iterative strategy is adopted, let $\hat{\mathbf{U}}_{p-1}$ represents the estimation of the signal subspace at the $(p-1)$-th iteration, then the estimation of noise covariance matrix at the p-th iteration can be written as

$$\hat{\mathbf{Q}}_p = \mathcal{D}(\hat{\mathbf{R}} - \hat{\mathbf{U}}_{p-1}\hat{\mathbf{U}}_{p-1}^H) \tag{18}$$

where $\mathcal{D}(\cdot)$ returns the diagonal matrix of the bracketed term and the estimate of $\mathbf{U}$ can be updated as

$$\hat{\mathbf{U}}_p = \hat{\mathbf{E}}_p \hat{\mathbf{\Sigma}}_p^{1/2} \tag{19}$$

where $\hat{\mathbf{\Sigma}}_p$ represents the diagonal matrix composed of the L largest eigenvalues from the eigenvalue decomposition (EVD) of $\hat{\mathbf{R}} - \hat{\mathbf{Q}}_p$, and $\hat{\mathbf{E}}_p$ denotes the corresponding eigenvectors. The iteration terminates when $\|\hat{\mathbf{U}}_p - \hat{\mathbf{U}}_{p-1}\|_F^2 \leq \vartheta$ or $\|\hat{\mathbf{Q}}_p - \hat{\mathbf{Q}}_{p-1}\|_F^2 \leq \vartheta'$, where ϑ or ϑ' is a small value defined by the user.

It is important to note that, according to the subspace theory, after performing the EVD of $\hat{\mathbf{R}} - \hat{\mathbf{Q}}_p$, the subspace spanned by the eigenvectors corresponding to the remaining small eigenvalues represents the noise subspace. Let $\hat{\mathbf{E}}'$ denote the estimate of such a subspace, consequently, DOAs can be determined by finding the L largest peaks in following MUSIC spectrum function:

$$\mathbf{P}_{MUSIC} = \frac{1}{\mathbf{a}^H(\theta,\phi)\hat{\mathbf{E}}'\hat{\mathbf{E}}'^H\mathbf{a}(\theta,\phi)} \tag{20}$$

where $\mathbf{a}(\theta,\phi), \theta \in [-180^\circ, 180^\circ], \phi \in [-90^\circ, 90^\circ]$ is the searching steering vector.

IV. Simulation Results

In this section, we validate the effectiveness of the proposed method by numerical simulations. The root-mean-square-error (RMSE) of DOA estimation obtained from 500 Monte-Carlo trials are used to evaluate the estimation performance. The user's transmit power is set to 1, and the path gain coefficient is randomly generated between 0 and -5 dB. The signal-to-noise ratio (SNR) and the worst noise power ratio (WNPR) in nonuniform noise are respectively defined as $\mathrm{SNR} = N^{-1}\sum_{n=1}^{N}\sigma_s^2/\sigma_n^2$ and $\mathrm{WNPR} = \sigma_{max}^2/\sigma_{min}^2$, where σ_s^2 denotes the signal power, σ_{max}^2 and σ_{min}^2 are the maximum and minimum values of the noise power, respectively. In the proposed method, $\alpha = \pi/8$, $\vartheta = 10^{-4}$ are preset, and $\hat{\mathbf{Q}}_0$ is initialized with $\mathcal{D}(\hat{\mathbf{R}})$.

In the first simulation, eight source signals are considered to impinge on the FA array at different angles, with the incident azimuth and elevation DOAs randomly generated from the range $[-50^\circ, 50^\circ]$. Without loss of generality, the movement pattern of the FA array is set to random movement, with the distance of each movement randomly generated within

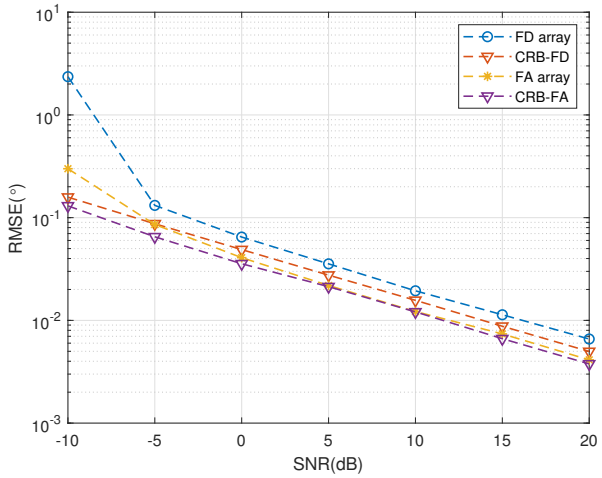

Fig. 2. RMSE of DOA estimation versus SNR.

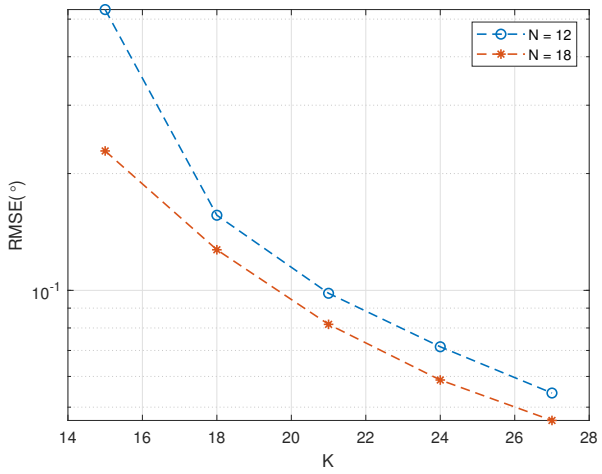

Fig. 3. RMSE of DOA estimation versus K.

the range of $[0.15\lambda, 0.45\lambda]$, and the number of movements is set to 24. The FA array is configured with 16 antennas, with 2 antennas arranged along the x-axis and 8 antennas along the z-axis. For comparison, a fixed fully-digital (FD) array with the same constrained area is also deployed, with element spacing set to half of the wavelength. As shown in Figure 2, the RMSE of both arrays steadily decreases with increasing SNR. In comparison, the FA array demonstrates significantly better estimation performance than the traditional FD array. This indicates that the FA array can greatly enhance the utilization efficiency of the spatial DoFs in the constrained area, while the hardware overhead of the designed FA array is much lower than that of the FD array.

In the second simulation, two FA arrays are configured with 12 and 18 FAs, respectively, to study the relationship between estimation performance and the number of movements. The other simulation configurations are the same as the first simulation. As shown in Figure 3, when the SNR is fixed at 0 dB, the RMSE steadily decreases as the number of movements increases, indicating that the FA array can fully utilize limited spatial DoFs. Furthermore, under the same number of movements, the performance of the 18-element FA array is significantly better than that of the 12-element FA array, suggesting that larger antenna arrays can perform spatial sampling more efficiently. Although increasing the number of antennas increases hardware costs, it clearly enhances the efficiency of spatial DoFs utilization, allowing for the full use of spatial DoFs in the constrained region with fewer movements. In this study, the FA array moves along only one dimension. However, it is foreseeable that a system where the FA array can move simultaneously in two dimensions will further improve estimation performance.

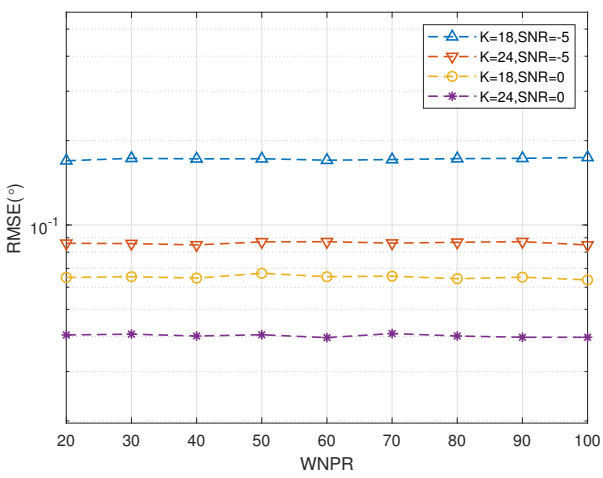

Fig. 4. RMSE of DOA estimation versus WNPR.

In the last simulation, by adjusting the number of movements and the SNR, we test the robustness of the proposed methods against the non-uniformity of sensor noises. The other simulation configurations are again the same as the first simulation. As shown in Figure 4, the performance of the proposed method remains nearly unchanged with the increase of WNPR under various configurations, showing its great robustness against nonuniform noise.

V. Conclusion

This paper has presented a high-precision DOA estimation method for FA array-assisted HAD architecture in the presence of nonuniform noise. In specific design, we adopt an array-level mobility approach to move to different positions for comprehensive spatial sampling and increased DoFs. Instead of using FA-HAD array output directly, an efficient strategy to reconstruct the large-scale SCM from the observed data is investigated, which provides an important guarantee for high-performance DOA estimation. Considering the impact of unknown nonuniform noise, the ILSSE technique combined with the MUSIC algorithm are jointly applied, which finally provide an improved DOA estimation result, as verified by simulations.

REFERENCES

[1] X. Chen, J. Tan, L. Kang, F. Tang, M. Zhao and N. Kato, "Frequency selective surface towards 6G communication systems: A contemporary survey," *IEEE Commun. Surveys Tuts.*, vol. 26, no. 3, pp. 1635–1675, Feb. 2024.

[2] Z. Wei, F. Liu, C. Masouros, N. Su, and A. P. Petropulu, "Toward multi-functional 6G wireless networks: Integrating sensing, communication, and security," *IEEE Commun. Mag.*, vol. 60, no. 4, pp. 65–71, Apr. 2022.

[3] K. Xu, X. Xia, C. Li, C. Wei, W. Xie and Y. Shi, "Channel feature projection clustering based joint channel and DoA estimation for ISAC massive MIMO OFDM system," *IEEE Trans. Veh. Technol.*, vol. 73, no. 3, pp. 3678–3689, Mar. 2024

[4] Z. Hu et al., "PRINCE: a pruned AMP integrated deep CNN method for efficient channel estimation of millimeter-wave and Terahertz ultra-massive MIMO systems," *IEEE Trans. Wireless Commun.*, vol. 22, no. 11, pp. 8066–8079, Nov. 2023.

[5] H. Li, J. Gong, and W. Cheng, "Hybrid beamforming design and signal processing with fully-connected architecture for mmWave integrated sensing and communications," *J. Commun. Inf. Netw.*, vol. 9, no. 2, pp. 151–161, Jun. 2024.

[6] S. Tarboush, A. Ali, and T. Y. Al-Naffouri, "Cross-field channel estimation for ultra massive-MIMO THz systems," *IEEE Trans. Wireless Commun*., vol. 23, no. 8, pp. 8619–8635, Aug. 2024.

[7] H. Hojatian, Z. Mlika, J. Nadal, J. -F. Frigon, and F. Leduc-Primeau, "Learning energy-efficient transmitter configurations for massive MIMO beamforming," *IEEE Trans. Mach. Learn. Commun. Netw*., vol. 2, pp. 939–955, Jun. 2024.

[8] Y. Chen, L. Yan, C. Han, and M. Tao, "Millidegree-level direction-of-arrival estimation and tracking for terahertz ultra-massive MIMO systems," *IEEE Trans. Wireless Commun*., vol. 21, no. 2, pp. 869–883, Feb. 2022.

[9] T. Wu, *et al.*. "Fluid antenna systems enabling 6G: Principles, applications, and research directions." *arXiv preprint*, arXiv:2412.03839, 2024.

[10] J. Yao, J. Zheng, T. Wu, M. Jin, C. Yuen, K.-K. Wong, and F. Adachi, "FAS-RIS communication: Model, analysis, and optimization," *IEEE Trans. Veh. Technol.*, early access, doi:10.1109/TVT.2025.3537294, 2025.

[11] Z. Xiao et al., "Channel estimation for movable antenna communication systems: A framework based on compressed sensing," *IEEE Trans. Wireless Commun.*, vol. 23, no. 9, pp. 11814–11830, Sep. 2024.

[12] W. Ma, L. Zhu and R. Zhang, "Compressed sensing based channel estimation for movable antenna communications," *IEEE Commun Lett.*, vol. 27, no. 10, pp. 2747–2751, Oct. 2023.

[13] J. Yao *et al.*, "Exploring Fairness for FAS-assisted Communication Systems: from NOMA to OMA," *IEEE Trans. Wireless Commun.*, early access, doi:10.1109/TWC.2025.3531056, 2025.

[14] J. Zheng T. Wu, X. Lai, C. Pan, M. Elkashlan, and K.-K. Wong, "FAS-assisted NOMA short-packet communication systems," *IEEE Trans. Veh. Technol.*, vol. 73, no. 7, pp. 10732–10737, Jul. 2024.

[15] W. Ma, L. Zhu and R. Zhang, "Movable antenna enhanced wireless sensing via antenna position optimization," *IEEE Trans. Wireless Commun.*, vol. 23, no. 11, pp. 16575–16589, Nov. 2024.

[16] J. Yao *et al.*, "FAS-driven spectrum sensing for cognitive radio networks," *IEEE Internet Things J.*, early access, doi:10.1109/JIOT.2024.3518623, 2024.

[17] J. Yao *et al.*, "Proactive monitoring via jamming in fluid antenna systems," *IEEE Commun. Lett.*, vol. 28, no. 7, pp. 1695–1702, Jul. 2024.

[18] H. Xu, M. Jin, Q. Guo, T. Jiang and Y. Tian, "Direction of arrival estimation with gain-phase uncertainties in unknown nonuniform noise," *IEEE Trans. Aerosp. Electron. Syst.*, vol. 59, no. 6, pp. 9686–9696, Dec. 2023.

[19] K. Guo, L. Zhang, Y. Li, T. Zhou and J. Yin, "Variational bayesian inference for DOA estimation under impulsive noise and nonuniform noise," *IEEE Trans. Aerosp. Electron. Syst.*, vol. 59, no. 5, pp. 5778–5790, Oct. 2023.

[20] C. Wen, X. Xie, and G. Shi, "Off-grid DOA estimation under nonuniform noise via variational sparse bayesian learning," *Signal Process.*, vol. 137, pp. 69–79, Aug. 2017.